Original Article

Cortical microinfarcts in memory clinic patients are associated with reduced cerebral perfusion

Doeschka A Ferro[1], Henri JJM Mutsaerts[2,3], Saima Hilal[4,5],
Hugo J Kuijf[6] ®, Esben T Petersen[7], Jan Petr[8] ®,
Susanne J van Veluw[9] ®, Narayanaswamy Venketasubramanian[10],
Tan Boon Yeow[11], Geert Jan Biessels[1] and Christopher Chen[5]

Abstract

Cerebral cortical microinfarcts (CMIs) are small ischemic lesions associated with cognitive impairment and dementia. CMIs are frequently observed in cortical watershed areas suggesting that hypoperfusion contributes to their development. We investigated if presence of CMIs was related to a decrease in cerebral perfusion, globally or specifically in cortex surrounding CMIs. In 181 memory clinic patients (mean age 72 ± 9 years, 51% male), CMI presence was rated on 3-T magnetic resonance imaging (MRI). Cerebral perfusion was assessed from cortical gray matter of the anterior circulation using pseudo-continuous arterial spin labeling parameters *cerebral blood flow* (CBF) (perfusion in mL blood/ 100 g tissue/min) and *spatial coefficient of variation* (CoV) (reflecting arterial transit time (ATT)). Patients with CMIs had a 12% lower CBF (beta $= -.20$) and 22% higher spatial CoV (beta $= .20$) (both $p < .05$) without a specific regional pattern on voxel-based CBF analysis. CBF in a 2 cm region-of-interest around the CMIs did not differ from CBF in a reference zone in the contralateral hemisphere. These findings show that CMIs in memory clinic patients are primarily related to global reductions in cerebral perfusion, thus shedding new light on the etiology of vascular brain injury in dementia.

Introduction

Cerebral cortical microinfarcts (CMIs) are small ischemic lesions visible on neuropathological examination and also detectable in vivo with high field strength magnetic resonance imaging (MRI).[1,2] CMIs commonly occur in patients with stroke and dementia and their contribution to vascular cognitive impairment is increasingly recognized.[3]

Although the pathophysiological mechanisms are not fully clear, CMIs probably have multiple causes.

[1]Department of Neurology, UMC Utrecht Brain Center, University Medical Center Utrecht, Utrecht, Netherlands
[2]Department of Radiology and Nuclear Medicine, Amsterdam University Medical Center, Amsterdam, Netherlands
[3]Department of Radiology, University Medical Center Utrecht, Utrecht, Netherlands
[4]Department of Radiology and Nuclear Medicine & Department of Epidemiology, Erasmus Medical Center, Rotterdam, Netherlands
[5]Memory Aging and Cognition Centre, Department of Pharmacology, National University of Singapore, Singapore, Singapore
[6]Image Sciences Institute, University Medical Center Utrecht, Utrecht, Netherlands
[7]Danish Research Centre for Magnetic Resonance, Centre for Functional and Diagnostic Imaging and Research, Copenhagen University Hospital Hvidovre, Copenhagen, Denmark
[8]Institute of Radiopharmaceutical Cancer Research, Helmholtz-Zentrum Dresden-Rossendorf, Dresden, Germany
[9]Department of Neurology, J.P.K. Stroke Research Center, Massachusetts General Hospital, Boston, USA
[10]Raffles Neuroscience Center, Raffles Hospital, Singapore, Singapore
[11]St. Luke's Hospital, Singapore, Singapore

Corresponding author:
Doeschka Ferro, Department of Neurology, University Medical Center Utrecht, Heidelberglaan 100, 3508 GA Utrecht, Netherlands.
Email: d.a.ferro@umcutrecht.nl

CMIs may result from small vessel disease (SVD), including cerebral amyloid angiopathy (CAA) and hypertensive SVD.[3] Moreover, CMIs can also result from thromboemboli due to large vessel or cardiac disease.[3,4] An interesting observation is that CMIs appear to be frequently located in the cortical watershed regions both in neuropathology[5–7] and MRI studies.[8,9] Watershed regions are located at the junction of two vascular territories and are therefore sensitive to hypoperfusion.[10] These findings suggest that hypoperfusion might play a role in the pathophysiology of CMIs.

Arterial spin labeling (ASL) is a non-invasive MRI perfusion technique, whereby blood is magnetically labeled in the cervical arteries. After a short post-labeling delay, a cerebral blood flow (CBF) map is obtained from the ASL signal in brain tissue.[36] Due to this fixed delay, the CBF maps may become inaccurate when blood flowing towards the brain is slowed – prolonged arterial transit time (ATT) – for example in elderly and patients with cerebrovascular disease.[11] Recently, the ASL-derived parameter *spatial coefficient of variation* (CoV) has been introduced that approximates ATT and is suitable for individuals with compromised CBF.[12]

In this study, we aim to determine if presence of CMIs is related to decreased cerebral perfusion, assessed with pseudo-continuous ASL (pCASL) CBF and spatial CoV in memory clinic patients; and if perfusion is specifically reduced locally around CMIs.

Methods

Population

This study involved patients who attended the memory clinics of the National University Hospital or St. Luke's Hospital in Singapore and had received one of the following diagnoses[13]: (1) *No cognitive impairment* (NCI): patients without objective cognitive impairment on formal neuropsychological tests or functional loss. (2) *Cognitive impairment – no dementia* (CIND) *with* (2 a) or *without* (2 b) *a history of stroke*: included patients who were impaired in at least one cognitive domain on neuropsychological testing, but did not meet the DSM (4th edition) criteria for dementia. Ischemic stroke was assessed based on medical history and confirmed by neuroimaging; patients with a hemorrhagic stroke were excluded from participation. Patients with dementia received an etiological diagnosis on the basis of internationally established criteria for (3) *Alzheimer dementia* (AD)[14] and (4) *Vascular dementia*.[15] Patients with other diagnoses (e.g. Frontotemporal Dementia), significant neurological comorbidities or loss of functional independence, were excluded from participation. All patients underwent a standardized clinical examination, 3-T MRI including ASL and neuropsychological testing.[4,13] For the present study, we included all patients recruited between December 2010 and September 2013 and had structural MRI and ASL sequences of sufficient quality.

Ethical approval for this study was obtained from the National Healthcare Group Domain-Specific Review Board (DSRB). The study was conducted in accordance with the Declaration of Helsinki. Written informed consent was obtained, in the preferred language of the patients, by bilingual study coordinators before recruitment into the study. Consent for patients lacking capacity was provided by their legal representative, as allowed by the DSRB.

Level of education was classified into four categories: no education, primary education, secondary education, or tertiary education. The following vascular risk factors were recorded: hypertension was defined as a previous diagnosis of hypertension, or use of antihypertensive medication; diabetes mellitus was defined as previous diagnosis of diabetes mellitus, or use of anti-diabetic medication; hyperlipidemia was defined as previous diagnosis of hyperlipidemia, or use of cholesterol-lowering medication. Obesity was defined as a body mass index >25. A history of cardiac disease was defined as a previous diagnosis of myocardial infarction, congestive heart failure, atrial fibrillation, or intervention procedures such as angioplasty, or stenting. A history of stroke was based on self-report.

MRI protocol

Patients were scanned on a 3-T MRI (Siemens Magnetom Trio Tim system) with a 32-channel receiver head-coil. The structural imaging protocol included a three-dimensional (3D) T1, 2D T2, T2*-weighted and fluid-attenuated inversion recovery (FLAIR) sequences (see eTable 2 for scanner-settings). pCASL images were acquired with labeling duration 1738 ms, post-labeling delay 1500 ms, and gradient-echo echo planar imaging of TR/TE 4000/9 ms, GRAPPA factor 3, $3.0 \times 3.0 \times 5.0\,mm^3$ voxels. ASL scans consisted of 23 pairs of images (control–labeled). CBF values were calculated voxel-wise from the mean differences of these two images. For each patient, the ASL protocol was carried out twice with a 1-h interval; CBF was averaged over the two sessions, unless one of the scan sessions was disregarded due to insufficient quality.

MRI ratings

The following MRI markers were rated: Microbleeds were assessed using the Brain Observer MicroBleed Scale.[16] The presence of large (i.e. >5 mm) cortical infarcts, subcortical infarcts (i.e. subcortical infarct

and/or lacunar infarcts), and white matter hyperintensities (WMHs) were rated according to the STRIVE criteria.[17] Infarct and WMH volumes were manually segmented on FLAIR and T1-weighted images using an in-house developed tool incorporated in MeVisLab (MeVis Medical Solutions AG, Bremen, Germany). Gray matter (GM), white matter, and cerebrospinal fluid were obtained from the T1-weighted image using the unified tissue segmentation approach[18] implemented in Statistical Parametric Mapping (SPM) (Wellcome Trust Centre for Neuroimaging, University College London, UK) from which total brain volume and intracranial volume were quantified. The presence of intracranial stenosis on the 3D time-of-flight MRA was defined as a narrowing exceeding 50% of the luminal diameter of the posterior cerebral, middle cerebral, and anterior cerebral artery and the intracranial part of vertebral, basilar, and internal carotid artery.[19]

CMIs were rated by visual inspection by a single experienced rater (SvV). In line with previously validated criteria, CMIs were obliged to be <5 mm in the largest dimension and hypointense on 3D T1-weighted images and hyperintense or isointense on FLAIR and T2-weighted images.[2] Lesions had to be strictly intracortical, perpendicular to the cortical surface and distinct from perivascular spaces. Moreover, a lesion was discarded as CMI if the area was considered part of a larger infarction. There was a good to excellent intra-rater agreement (Intraclass correlation coefficient = 0.97; Dice's similarity coefficient = 0.65) on the CMI ratings of this cohort. We have previously published the clinical correlates of CMIs in this specific cohort.[13] A 3D representation of all CMIs in the cohort was configured by registering the lesions to the MNI152 standard brain (Figure 1). We used an in-house developed watershed atlas as overlay. This atlas was based on the average territorial ASL maps from individuals with steno-occlusive disease.[20] The watershed areas were defined as overlapping perfusion territories across subjects.

ASL

ASL post-processing was performed with the *ExploreASL* toolbox, an in-house developed toolbox based on SPM and Matlab7.12.0 (MathWorks, Nattick, MA).[21] Post-processing included motion correction and rigid body registration of the CBF map to a GM map and normalized into common space through the T1-weighted images using Diffeomorphic Anatomical Registration analysis using Exponentiated Lie algebra (DARTEL)[22] using CAT12.[23] From the CBF map, two ASL parameters were acquired within a pGM > 0.7 GM region-of-interest (ROI): CBF and Spatial CoV. CBF reflects perfusion in mL blood/


Figure 1. 3D representation of cerebral cortical microinfarcts with watershed overlay. Superior view of a 3D representation of cerebral cortical microinfarcts (black dots) in the cohort projected on an MNI-standard brain. The red overlay signifies the cortical watershed regions.[20]

100 g tissue/min. To avoid systematic bias in patients with more severe atrophy, partial volume corrections was applied to the CBF (CBF_{pvc}) using local linear regression within a 3D kernel based on the CAT12 tissue partial volume maps.[24] Spatial CoV is a novel ASL parameter particularly suitable for individuals with severely prolonged ATT, such as patients with a vascular brain disease in which CBF sometimes cannot be readily measured. It serves as a proxy of ATT and is calculated by dividing the SD of the CBF by the mean CBF. Additional details regarding spatial CoV have been published previously.[12]

Global CBF and spatial CoV were obtained using a GM mask of anterior brain circulation only (i.e. the internal carotid artery flow territory, not the posterior circulation as supplied by the vertebrobasilar system), as acquisition parameters were not favorable for the longer arrival time in the posterior circulation. Mean cortical GM CBF was calculated from the intersection of the watershed ROI obtained from a watershed atlas[20] – shown in Figure 1 – and the subject-wise GM mask. A voxel-based analysis of the cortical GM CBF differences between patients with and without CMIs was performed in SPM. CBF maps were smoothed with a 6-mm full width at half maximum Gaussian kernel.

Individual CMI ROIs composed of a 2-cm diameter sphere around the CMIs. The diameter was set at 2 cm, as a trade-off between spatial specificity requiring the smallest possible diameter and signal to noise ratio/resolution of ASL, which puts boundaries to the minimum diameter that can be used. Within the sphere only the cortical GM was considered for partial volume corrected CBF assessment. A comparative ROI was created on the same anatomical location in the contralateral hemisphere. CMI ROIs were excluded from analysis if they overlapped (either in the ipsi- or contralateral hemisphere) with another ROI or larger infarct, resulting in a total of 67 CMI ROIs in 35 patients. Figure 2 provides a visual representation of the ROI analysis.

Visual quality assessment of the ASL scans was performed by two independent raters (DF and HM) based on visual evaluation. Scans were classified according to one of four categories (Figure 3): (1) *Unusable* was applied to scans that were incomplete, had labeling errors, or severe motion artifacts (n = 53). (2) *Angiogram* for scans with predominantly vascular contrast and no or minimal tissue perfusion (n = 33).[12] (3) *Acceptable* scans which had minor vascular contrast or motion artifacts and reasonable tissue perfusion (n = 58), or (4) *good* (n = 90). Patients with unusable scans were excluded from analysis. All other patients were analyzed, but the 33 patients with *angiogram*-classified ASL scans were not included in the CBF analysis, as the lack of tissue perfusion causes unreliable interpretation.[12]

Statistical analysis

Differences in baseline characteristics between patients with and without CMIs were compared with an independent t-test (for continuous normally distributed data), χ-square test (for proportions), and Mann–Whitney U test (for continuous, non-normally distributed data). WMH volume and spatial CoV data were log transformed. The relation between CMI presence (independent variable) and CBF, CBF_{pvc}, and spatial CoV (dependent variable) was assessed using linear regression in model 1. In model 2, age and sex were entered as covariates. In model 3, we performed additional explorative analyses where individual and combined vascular risk factors were added as covariates to model 2 and in model 4 where individual and combined neuro-imaging markers were added as covariates to model 2. Models are presented with B-values representing the mean difference (and 95% confidence interval) in cerebral perfusion between patients with and without CMIs. Within the patients with CMIs, Spearman's rank correlation was used to determine the relationship between the


N	ASL quality	Defined by	Example scans
53 (23%)	Unusable	Incomplete protocol, labeling errors or severe motion artifacts	
33 (14%)	Angiogram	Predominantly vascular contrast, no or minimal tissue perfusion	
58 (25%)	Acceptable	Minor vascular contrast or movement artefacts, reasonable tissue perfusion	
90 (38%)	Good	Scans without vascular contrast	
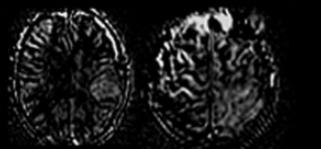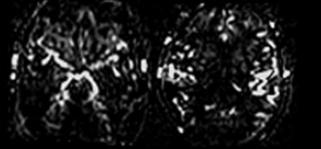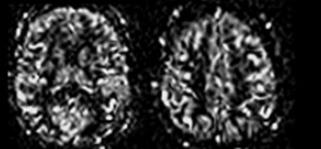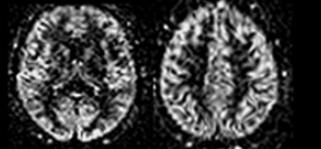
Figure 2. Quality assessment method of the ASL scans, including quality criteria and example images.
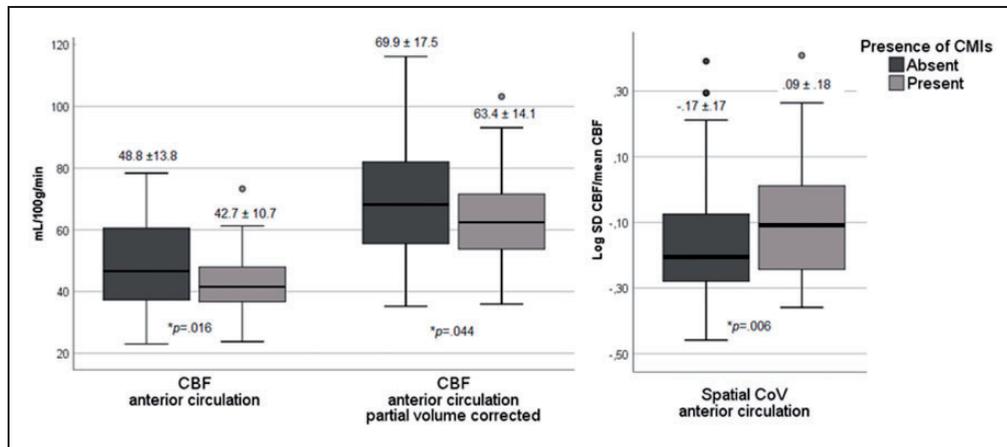
Figure 3. Cerebral perfusion in patients with and without cerebral cortical microinfarcts (CMIs). Boxplots of the mean and standard deviation of the cerebral blow flow (CBF), partial volume corrected CBF and spatial coefficient of variation (CoV) in the anterior circulation in patients with and without CMIs. P-values are reported on the uncorrected differences between patients with and without CMIs.

total number of CMIs per patient to the CBF, CBF_{pvc}, and spatial CoV. For the voxel-based analysis, significant clusters of voxels were identified using a primary cluster-forming threshold of $p < .001$, family-wise corrected for cluster sizes corresponding to $p < 0.05$. For the CMI ROI analysis, CBF was compared between the ROIs in the ipsi- and contralateral hemispheres in a paired (within subjects) t-test. All data were analyzed using IBM SPSS statistics (version 25) and a p-value $< .05$ was considered statistically significant.

Results

Demographics and CMI occurrence

Of the 234 patients, 53 (23%) were excluded due to insufficient quality of the ASL scan. The excluded patients were on average older and had more severe cognitive impairment (i.e. a lower mini-mental state examination and a higher proportion of patients with diagnosis dementia) and a higher CMI burden (eTable 1). Of the remaining 181 patients included in the spatial CoV analyses, 148 patients – without angiogram like ASL scans – were suitable for CBF analyses. The mean age of these 181 patients was 72 years (SD 9), 51% were male and the majority (80%) of Chinese ethnicity. Of these patients, 41% was diagnosed with dementia, 43% with CIND, and 16% with NCI. The 33 patients who were unsuitable for the CBF analysis due to angiogram qualified ASL scans had a higher proportion of males and a higher CM burden (eTable 1).

A total of 179 CMIs were detected in 50 (28%) of the 181 patients. The number of CMIs per patient ranged between 1 and 43, and 23 patients (46%) had multiple CMIs. Patients with CMIs were proportionally often

male ($p = .063$) and had a higher burden of vascular risk factors and cerebrovascular disease (Table 1). Figure 1 displays a 3D spatial topographical representation of all CMIs in the cohort. Visual inspection suggests a clustering of CMIs in fronto-parietal areas without evident predilection for the cortical watershed regions.

Perfusion in patients with and without CMIs

CMI presence was associated with a 12% reduced cortical CBF (effect size d = 0.49, $p = .016$), a 9% reduced partial volume corrected CBF (CBF_{pvc}) (effect size d = 0.41, $p = .044$) and a 22% increased spatial CoV (effect size d = 0.46, $p = .006$) in the anterior circulation (Figure 4; Table 2 model 1). When corrected for age and sex, results remained similar for CBF ($p = .038$) and spatial CoV ($p = .039$), but attenuated for CBF_{pvc} ($p = .078$) (Table 2 model 2). The individual and combined vascular risk factors had a marginal effect on the relationship between CMI presence and cerebral perfusion (Table 2 model 3). Similarly, the individual neuro-imaging markers, including intracranial stenosis, also had a marginal effect on the relationship between CMIs presence and cerebral perfusion, with the exception of total brain volume and WMHs that both attenuated the strength of the association between CMIs and perfusion measures (Table 2 model 4). Moreover, in the model with all neuro-imaging markers combined, the relationship between CMI and perfusion measures disappeared. Within the patients with CMIs, a higher number of CMIs per patient was modestly correlated to a higher spatial CoV (Rho = .27, $p = .057$), but not to CBF (Rho = −.06, $p = .752$) or CBF_{pvc} (Rho = −.07, $p = .699$). With respect to the perfusion in the watershed

Table 1. Baseline characteristics of patients with and without CMIs.

	CMI absent (N = 131)	CMI Present (N = 50)	p
Age, mean (SD), years	71.5 (9.3)	72.6 (8.8)	.464
No. (%) males	61 (47)	31 (62)	.063
Ethnicity, no. (%) Chinese	107 (82)	37 (74)	.251
Education, median (IQR) (4 levels)	2 (1–3)	2 (1–3)	.357
Vascular risk factors			
Hypertension, no. (%)	92 (70)	43 (86)	.029
Hypercholesterolemia, no. (%)	82 (63)	44 (88)	.001
Diabetes, no. (%)	46 (35)	25 (50)	.067
Current smoking, no. (%)	11 (8)	7 (14)	.260
Obesity (4 missing), no. (%)	4 (3)	5 (10)	.062
History of stroke, no. (%)	44 (34)	25 (50)	.042
Cardiac disease, no. (%)	19 (15)	20 (40)	<.001
Cognitive performance			
CDR median (IQR)	0.5 (0–1)	0.75 (0.5–1)	.238
MMSE, mean (SD)	22.1 (5.8)	20.6 (5.8)	.129
Clinical diagnosis, no. (%)			
NCI	25 (19)	4 (8)	.135
CIND	56 (43)	21 (42)	
Dementia	50 (38)	25 (50)	
Neuro-imaging markers			
Total brain volume, mean (SD), % of TIV	64.8 (5.7)	62.1 (6.2)	.006
WMH volume, median (IQR), mL	8.3 (3.3–19.8)	12.1 (5.4–29.7)	.010 [a]
Presence of cortical infarcts >5 mm, no. (%)	8 (6)	17 (34)	<.001
Presence of subcortical infarcts, no. (%)	32 (24)	22 (44)	.010
Presence of microbleeds, no. (%)	66 (50)	35 (70)	.017
Presence intracranial stenosis (4 missing)	23 (18)	15 (31)	.053

CMI: cerebral cortical microinfarct; CDR: clinical dementia rating scale; MMSE: mini-mental state examination; NCI: no cognitive impairment; CIND: cognitive impairment – no dementia; TIV: total intracranial volume; WMH: white matter hyperintensity. Obesity was defined as a body mass index >25.
[a]WMH volume was entered into the analysis after a logarithmic transformation of the data.
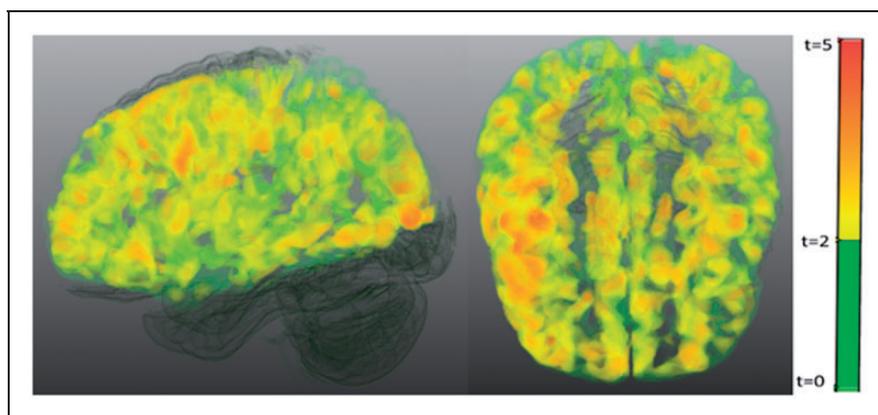

Figure 4. Voxel based analysis of the differences in cerebral blood flow between the group of patients with cortical microinfarct compared to the group of patients without cortical microinfarcts. Significant clusters (cluster threshold of p<.001, family wise corrected to <0.05) are shown in yellow to red, non-significant clusters are shown in green.

Table 2. Association between CMI presence and cerebral perfusion adjusted for covariates.

	CBF (N = 148) B (95% CI)	p	CBF$_{pvc}$ (N = 148) B (95% CI)	p	Spatial CoV (N = 181) B (95% CI)	p
Model 1: CMI presence	−6.1 (−11.1; −1.2)	.016	−6.5 (−12.9; −.2)	.044	.08 (.02; .14)	.006
Model 2: CMI + age, sex	−5.0 (−9.7; −.2)	.038	−5.6 (−11.9; .6)	.078	.06 (.003; .11)	.039
Model 3: CMI + age, sex +						
Hypertension	−4.6 (−9.3; .1)	.054	−5.1 (−11.4; 1.1)	.106	.05 (−.005; .10)	.079
Hypercholesterolemia	−4.4 (−9.3; .4)	.073	−4.8 (11.2; 1.6)	.143	.05 (−.006; .10)	.082
Diabetes	−4.5 (−9.3; .2)	.061	−5.3 (−11.7; 1.0)	.098	.06 (.003; .11)	.040
Current smoking	−5.2 (−9.9; −.4))	.033	5.8 (−12.1; .5)	.072	.05 (.001; .11)	.045
Obesity	−5.0 (−9.9; −.1)	.044	−6.2 (−12.7; .4)	.064	.06 (.004; .11)	.034
History of stroke	−5.7 (−10.5; −1.0)	.018	−4.9 (−11.2; 1.4)	.126	.05 (.001; .11)	.047
Cardiac disease	−4.5 (−9.2; .3)	.065	−6.4 (−12.7; −.1)	.048	.05 (−.01; .10)	.122
All vascular risk factors	−4.8 (−9.8; .3)	.066	−5.7 (−12.5; 1.0)	.096	.05 (−.005; .11)	.075
Model 4: CMI + age, sex +						
Total brain volume	−3.7 (−8.2; .8)	.110	−4.5 (−10.7; 1.7)	.154	.04 (−.01; .10)	.104
WMH volume[a]	−3.1 (−7.8; 1.7)	.200	−3.6 (−10.0; 2.8)	.265	.03 (−.02; .09)	.210
Presence of cortical infarcts	−5.0 (−10.0; −.1)	.045	−5.6 (−12.2; .9)	.090	.05 (−.003; .11)	.064
Presence of subcortical infarcts	−4.6 (−9.5; .2)	.059	−5.0 (−11.4; 1.4)	.122	.05 (−.001; .11)	.048
Presence of microbleeds	−4.2 (−8.9; .6)	.086	−4.4 (−10.7; 1.9)	.171	.05 (−.004; .10)	.069
Presence intracranial stenosis	−4.4 (−9.2; .4)	.073	−5.0 (−11.4; 1.5)	.128	.05 (−.003; .10)	.064
All imaging markers	−1.1 (−6.0; 3.9)	.670	−1.2 (−8.1; 5.6)	.727	.02 (−.04; .07)	.581

CBF: cerebral blood flow; CBF$_{pvc}$: partial volume corrected cerebral blood flow; spatial CoV: spatial coefficient of variation of the cerebral blood flow; CMI: cerebral cortical microinfarct; WMH: white matter hyperintensity. Data presented as B: mean difference between patients with and without CMIs and the 95% confidence interval. Model 1: unadjusted; model 2: adjusted for age and sex; model 3: adjusted for age, sex and each individual vascular risk factor added separately; model 4: adjusted for age, sex and each individual neuro-imaging marker added separately.
[a]WMH volume was entered into the analysis after a logarithmic transformation of the data.

regions, the difference in CBF (beta = −.17, $p < .05$) and CBF$_{pvc}$ (beta = −.16, $p = .058$) between patients with and without CMIs in these regions was of similar magnitude as the whole anterior brain circulation. To determine the spatial pattern of hypoperfusion in patients with CMIs compared to patients without CMIs, a voxel-based analysis of CBF signal was performed, which showed a relatively homogeneous pattern of hypoperfusion over the whole cortex (Figure 5).

Perfusion around CMIs

Mean CBF in 2-cm cortical GM ROIs around the CMIs (CBF = 73.1 mL/100 g tissue/min, SD 26.7) was not different from the CBF of the ROI in the contralateral reference regions (CBF = 73.0 mL/100 g tissue/min, SD 28.6) ($p = .97$).

Discussion

We found that presence of CMIs in memory clinic patients was associated with reduced cerebral perfusion throughout the anterior circulation, but that perfusion in the cortex directly surrounding CMIs was not specifically affected.
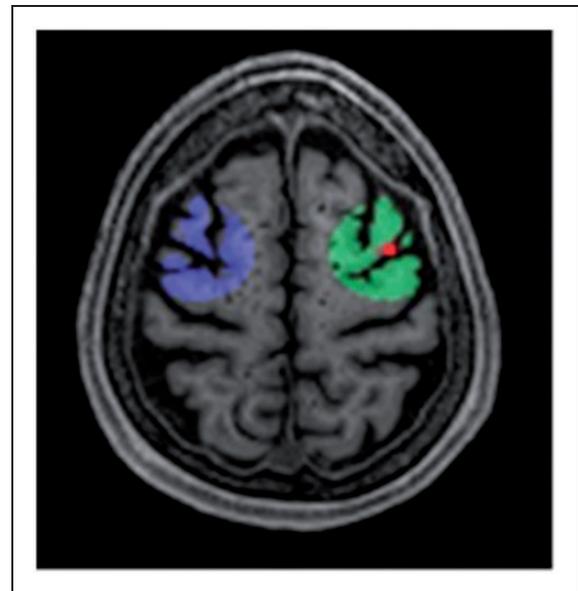

Figure 5. Local CBF analysis using CMI ROIs. Cerebral blood flow (CBF) within a Region-of-Interest (ROI), composed of a 2cm diameter sphere (green area) around the cortical microinfarcts (CMIs) (red dot), was compared to the CBF within an ROI on the same anatomical location in the contralateral hemisphere (purple area).

The two ASL parameters studied (i.e. CBF and spatial CoV) congruently showed that cerebral perfusion was affected in patients with CMIs. Previous studies had already provided circumstantial evidence of a link between CMIs and perfusion. Post-mortem subcortical CMIs were found to relate to ante-mortem blood pressure decline on serial blood pressure assessments, possibly translating in reduced cerebral perfusion pressure.[25] Furthermore, both post-mortem[5–7] and MRI studies[8,9] have suggested that CMIs might have a predilection for the cortical watershed areas. This hypothesis could, however, not be confirmed in the current study. Although clustered in the fronto-parietal cortex, we observed no evident predilection of CMIs in the watershed areas, as defined by a previously established ASL atlas. These different findings might be attributed to the study population, as both CMI occurrence and etiology are known to vary in different contexts. Additionally, previous neuropathological studies[5–7] allow for detection of much smaller (i.e. <1 mm) CMIs that could have a different topographical localization. Future research is encouraged to further explore this on ultra-high field MRI, which allows for detection of intermediate size CMIs.

In line with our observations in CMIs, the presence of other manifestations of SVD on MRI has been linked to reductions in cerebral perfusion. There is, for example, a growing body of – mostly cross-sectional – studies reporting a relation between WMHs and reduced perfusion.[26] Of note, perfusion is also found to be locally reduced within WMH lesions[27] and longitudinal studies suggested that hypoperfusion probably precedes the formation of WMHs.[28,29] The presence of microbleeds is also reported to be related to globally reduced perfusion.[30] Although we are not aware of studies exploring perfusion directly around the microbleeds, the previous study indicates that hypoperfusion is not restricted to the preferential parietal–occipital location of cortical microbleeds in CAA.

Although perfusion may be reduced at the lesion sites, particular for WMHs, the consistent finding for the different manifestations of SVDs is that they predominantly associate with globally reduced cerebral perfusion. The question is therefore what mechanisms tie these small focal lesions to reduced global perfusion. First, there could be a causal link, where hypoperfusion directly induces CMIs. In that scenario, CMIs may occur at sites that reach a critical perfusion threshold or that are exposed to a second pathophysiological mechanism. Disturbances more proximal in the vascular tree, such as cardiac pump dysfunction[4] or stenosis or occlusion of the cervical and intracranial arteries,[13,31] could certainly contribute towards reaching a critical perfusion threshold. In this study, we found a marginal effect of intracranial stenosis on the relation between CMIs presence and perfusion. Unfortunately, no data on extracranial stenosis or cardiac pump function were available in this cohort. Evidence for an interaction with a second pathophysiological mechanism comes from a CAA mouse model study, which showed that mice subjected to chronic hypoperfusion not only showed accelerated deposition of leptomeningeal amyloid but also a markedly higher CMI burden than CAA mice with normal cerebral perfusion.[32]

Another possibility is that both reduced perfusion and CMIs are due to shared etiologies, without being directly causally linked to each other. Such shared etiologies could include SVD, where restriction of vessel lumen by arteriolosclerosis, CAA, loss of autoregulation, blood–brain barrier leakage, and inflammation could affect perfusion as well as induce CMIs.[33] Explorative analysis in this study showed that entering other imaging manifestations of SVDs, especially WMHs, together with CMIs in the statistical models, attenuated the association between CMI presence and perfusion. Even shared vascular risk factors, such as hypertension, could contribute to both independently. However, our exploratory analyses indicated that both individual and combined vascular risk factors only marginally affected the relationship between CMIs and perfusion. It is highly likely that the abovementioned mechanisms coincide and even interact. For example, it has been suggested that reduced arterial flow can prompt the formation of thrombo-emboli due to impaired wash-out,[34] providing additional mechanisms for CMI development. We therefore encourage future studies to further investigate the underlying mechanisms tying CMIs to cerebral perfusion. This could include zooming in on clinical populations known to exhibit compromised cerebral perfusion, such as patients with heart failure or severe carotid artery stenosis. Moreover, the mediating role of SVDs could be further explored by assessing interrelations with other imaging manifestations of SVDs, in particular WMH, but also by using novel measures of small vessel function and blood–brain barrier function, that may provide more direct indications of the condition of the small vessels in SVD, independent of downstream lesions.[35]

The interaction between CMIs and reduced cerebral perfusion clearly carries clinical significance. Over the years, a robust relationship has been demonstrated between CMIs and cognitive impairment, yet currently without clear prospect of treatment.[3] The current study highlights the importance of cerebral perfusion as potential therapeutic target.

This study has several strengths and limitations. It involved a heterogeneous memory clinic cohort with a broad range of cognitive symptoms, strengthening results as it reflects daily clinical practice. Although CMIs were rated according to validated criteria, the limited sensitivity of 3-T MRI needs to be acknowledged, as it allows detection of only a fraction of the CMIs visible on 7-T or neuropathological examination.[2] It remains unclear how these smaller CMIs relate to cerebral perfusion. A watershed atlas based on a group-averaged territorial ASL map was used in this study. However, it must be acknowledged that there is a large inter-individual variation in the size and exact location of the watershed regions. Major challenges of the ASL technique include a low signal-to-noise ratio and problematic application in patients with prolonged ATT.[36] As a result, we applied relatively large ROIs of 2 cm around the CMIs, while the area of perfusion restriction could in fact be smaller. Finally, we had to exclude a relatively high (23%) proportion of severely affected patients due to poor ASL scan quality. We partially resolved this issue by using the novel ASL parameter spatial CoV and improve ASL quality by repeating the ASL protocol twice.

Conclusion

CMI presence was associated with decreased cerebral perfusion in the anterior circulation of memory clinic patients, but perfusion in the region directly surrounding CMIs did not appear selectively affected. Hence, in line with other manifestations of SVDs, CMIs predominantly relate to a global reduction in perfusion. This could be the result of a direct causal relation of hypoperfusion on CMI development or shared underlying mechanisms, such as SVD, proximal vascular pathology, and vascular risk factors, or a combination of all. Further unravelling the link between CMIs and perfusion reduction will significantly contribute to understanding of vascular cognitive impairment and has important clinical implications with respect to treatment.

Authors' contributions

Study concept and design: DF, HM, SH, GB, CC.
Acquisition, analysis, or interpretation of data: DF, HM, SH, HK, EP, JP, SV, NV, TY, GB, CC.
Drafting of the manuscript: DF, GB, CC.
Critical revision of the manuscript for important intellectual content: DF, HM, SH, HK, EP, JP, SV, NV, TY, GB, CC.
Statistical analysis: DF, HM.
Obtained funding: GB, CC.
CC had full access to all the data in the study and takes responsibility for the integrity of the data and the accuracy of the data analysis.

ORCID iD

Hugo J Kuijf https://orcid.org/0000-0001-6997-9059
Jan Petr https://orcid.org/0000-0002-3201-6002
Susanne J van Veluw https://orcid.org/0000-0002-7957-8643

Supplemental material

Supplemental material for this paper can be found at the journal website: http://journals.sagepub.com/home/jcb

References

1. Smith EE, Schneider JA, Wardlaw JM, et al. Cerebral microinfarcts: the invisible lesions. *Lancet Neurol* 2012; 11: 272–282.
2. Van Veluw SJ, Zwanenburg JJM, Engelen-Lee J, et al. In vivo detection of cerebral cortical microinfarcts with high-resolution 7T MRI. *J Cereb Blood Flow Metab* 2013; 33: 322–329.
3. van Veluw SJ, Shih AY, Smith EE, et al. Detection, risk factors, and functional consequences of cerebral microinfarcts. *Lancet Neurol* 2017; 16: 730–740.
4. Hilal S, Chai YL, van Veluw S, et al. Association between subclinical cardiac biomarkers and clinically manifest cardiac diseases with cortical cerebral microinfarcts. *JAMA Neurol* 2017; 74: 403.
5. Kapasi A, Leurgans SE, James BD, Boyle PA, Arvanitakis Z, Nag S, et al. Watershed microinfarct pathology and cognition in older persons. *Neurobiol Aging* 2018; 70: 10–17.
6. Suter OC, Sunthorn T, Kraftsik R, et al. Cerebral hypoperfusion generates cortical watershed microinfarcts in Alzheimer disease. *Stroke* 2002; 33: 1986–1992.
7. Strozyk D, Dickson DW, Lipton RB, et al. Contribution of vascular pathology to the clinical expression of dementia. *Neurobiol Aging* 2010; 31: 1710–1720.
8. Ferro DA, Van Veluw SJ, Koek HL, et al. Cortical cerebral microinfarcts on 3 Tesla MRI in patients with vascular cognitive impairment. *J Alzheimer's Dis* 2017; 60: 1443–1450.

9. Riba-Llena I, Koek M, Verhaaren BFJ, et al. Small cortical infarcts: prevalence, determinants, and cognitive correlates in the general population. *Int J Stroke* 2015; 10: 18–24.

10. Bladin CF and Chambers BR. Clinical features, pathogenesis, and computed tomographic characteristics of internal watershed infarction. *Stroke* 1993; 24: 1925–1932.

11. Dai W, Fong T, Jones RN, et al. Effects of arterial transit delay on cerebral blood flow quantification using arterial spin labeling in an elderly cohort. *J Magn Reson Imaging* 2017; 45: 472–481.

12. Mutsaerts HJ, Petr J, Václavů L, et al. The spatial coefficient of variation in arterial spin labeling cerebral blood flow images. *J Cereb Blood Flow Metab* 2017; 37: 3184–3192.

13. van Veluw SJ, Hilal S, Kuijf HJ, et al. Cortical microinfarcts on 3T MRI: clinical correlates in memory-clinic patients. *Alzheimer's Dement* 2015; 11: 1500–1509.

14. McKhann G, Drachman D, Folstein M, et al. Clinical diagnosis of Alzheimer's disease: report of the NINCDS-ADRDA Work Group under the auspices of Department of Health and Human Services Task Force on Alzheimer's Disease. *Neurology* 1984; 34: 939–944.

15. Wiederkehr S, Simard M, Fortin C, et al. Comparability of the clinical diagnostic criteria for vascular dementia: a critical review. *Part I*. J Neuropsychiatry Clin Neurosci 2008; 20: 150–161.

16. Cordonnier C, Potter GM, Jackson CA, et al. Improving interrater agreement about brain microbleeds: development of the Brain Observer MicroBleed Scale (BOMBS). *Stroke* 2009; 40: 94–99.

17. Wardlaw JM, Smith EE, Biessels GJ, et al. Neuroimaging standards for research into small vessel disease and its contribution to ageing and neurodegeneration. *Lancet Neurol* 2013; 12: 822–838.

18. Ashburner J and Friston KJ. Unified segmentation. *Neuroimage* 2005; 26: 839–851.

19. Hilal S, Xu X, Ikram MK, et al. Intracranial stenosis in cognitive impairment and dementia. *J Cereb Blood Flow Metab* 2017; 37: 2262–2269.

20. Hartkamp NS, Petersen ET, Chappell MA, et al. Relationship between haemodynamic impairment and collateral blood flow in carotid artery disease. *J Cereb Blood Flow Metab* 2018; 38: 2021–2032.

21. Mutsaerts HJMM, Petr J, Thomas DL, et al. Comparison of arterial spin labeling registration strategies in the multi-center GENetic frontotemporal dementia initiative (GENFI). *J Magn Reson Imaging* 2018; 47: 131–140.

22. Ashburner J. A fast diffeomorphic image registration algorithm. *Neuroimage* 2007; 38: 95–113.

23. Gaser C and Dahnke R. CAT – a computational anatomy toolbox for the analysis of structural MRI data. In: *22nd annual meeting of the organisation for human brain mapping*, Geneva, Switzerland. 2016.

24. Asllani I, Borogovac A and Brown TR. Regression algorithm correcting for partial volume effects in arterial spin labeling MRI. *Magn Reson Med* 2008; 60: 1362–1371.

25. Graff-Radford J, Raman MR, Rabinstein AA, et al. Association between microinfarcts and blood pressure trajectories. *JAMA Neurol* 2018; 75: 212–218.

26. Shi Y, Thrippleton MJ, Makin SD, et al. Cerebral blood flow in small vessel disease: a systematic review and meta-analysis. *J Cereb Blood Flow Metab* 2016; 36: 1653–1667.

27. Brickman AM, Zahra A, Muraskin J, et al. Reduction in cerebral blood flow in areas appearing as white matter hyperintensities on magnetic resonance imaging. *Psychiatry Res Neuroimaging* 2009; 172: 117–120.

28. Promjunyakul NO, Dodge HH, Lahna D, et al. Baseline NAWM structural integrity and CBF predict periventricular WMH expansion over time. *Neurology* 2018; 90: e2107–e2118.

29. Bernbaum M, Menon BK, Fick G, et al. Reduced blood flow in normal white matter predicts development of leukoaraiosis. *J Cereb Blood Flow Metab* 2015; 35: 1610–1615.

30. Gregg NM, Kim AE, Gurol ME, et al. Incidental cerebral microbleeds and cerebral blood flow in elderly individuals. *JAMA Neurol* 2015; 15213: 1021–1028.

31. Dieleman N, van der Kolk AG, Zwanenburg JJ, et al. Relations between location and type of intracranial atherosclerosis and parenchymal damage. *J Cereb Blood Flow Metab* 2016; 36: 1271–1280.

32. Okamoto Y, Yamamoto T, Kalaria RN, et al. Cerebral hypoperfusion accelerates cerebral amyloid angiopathy and promotes cortical microinfarcts. *Acta Neuropathol* 2012; 123: 381–394.

33. Pantoni L. Cerebral small vessel disease: from pathogenesis and clinical characteristics to therapeutic challenges. *Lancet Neurol* 2010; 9: 689–701.

34. Caplan LR, Wong KS, Gao S, et al. Is hypoperfusion an important cause of strokes? If so, how? *Cerebrovasc Dis* 2006; 21: 145–153.

35. Zwanenburg JJM and van Osch MJP. Targeting cerebral small vessel disease with MRI. *Stroke* 2017; 48: 3175–3182.

36. Alsop DC, Detre JA, Golay X, et al. Recommended implementation of arterial spin-labeled perfusion MRI for clinical applications: a consensus of the ISMRM perfusion study group and the European consortium for ASL in dementia. *Magn Reson Med* 2015; 73: 102–116.